TOWARD A MESOSCALE HYDROLOGICAL AND MARINE METEOROLOGICAL OBSERVATION NETWORK IN THE SOUTH CHINA SEA

BY LEI YANG, DONGXIAO WANG, JIAN HUANG, XIN WANG, LILI ZENG, RUI SHI, YUNKAI HE, QIANG XIE, SHENGAN WANG, RONGYU CHEN, JINNAN YUAN, QIANG WANG, JU CHEN, TINGTING ZU, JIAN LI, DANDAN SUI, AND SHIQIU PENG

A three-dimensional mesoscale hydrological and marine meteorological observation network can advance research on air–sea interaction in the South China Sea.

The South China Sea (SCS) is the largest semi-enclosed marginal sea in the tropical western Pacific and is surrounded by densely populated Asian countries. The SCS throughflow, colder and saltier water entering the SCS through the Luzon Strait, and warmer and fresher water exiting through the Mindoro and Karimata Straits constitute the most important circulation in the SCS and one that plays an important role in modulating the variation of the Asian monsoon and El Niño–Southern Oscillation (ENSO) (Qu et al. 2005, 2006). The SCS throughflow acts as a heat and freshwater conveyor, transferring up to 0.1–0.2 PW of heat and 0.1 Sverdrups (Sv; 1 Sv $\equiv 10^6$ m^3 s^{-1}) of freshwater from the SCS into the Indonesian Sea and tropical Indo-Pacific Ocean (Qu et al. 2006). It is likely responsible for the subsurface maximum velocity in the Makassar Strait and significantly reduces the Indonesian Throughflow heat transport (Qu et al. 2005; Liu et al. 2006; Tozuka et al. 2007), thus having a potential impact on the heat distribution in the Maritime Continent and tropical Indo-Pacific Ocean (Qu et al. 2006).

Driven by seasonal monsoonal winds, the upper-layer circulation over the deep basin of the SCS displays a basinwide cyclonic circulation in winter and a cyclonic northern gyre and anticyclonic southern gyre during summer (Hu et al. 2000; Qu 2000; Su 2004; Fang et al. 2002; Gan et al. 2006; Dippner et al. 2007; Gan and Qu 2008). Under the forcing of monsoon and complex topography, the SCS is characterized by high mesoscale eddy activity

AFFILIATIONS: YANG, D. WANG, X. WANG, ZENG, SHI, HE, S. WANG, R. CHEN, Q. WANG, J. CHEN, ZU, LI, SUI, and PENG—State Key Laboratory of Tropical Oceanography, South China Sea Institute of Oceanology, Chinese Academy of Sciences, Guangzhou, China; HUANG AND YUAN—Guanghou Institute of Tropical and Marine Meteorology, China Meteorology Administration, Guangzhou, China; XIE—Sanya Institute of Deep Sea Science and Engineering, Chinese Academy of Sciences, Guangzhou, China
CORRESPONDING AUTHOR: Dongxiao Wang, South China Sea Institute of Oceanology, Chinese Academy of Sciences, 164 West Xingang Rd., Haizhu District, Guangzhou 510301, China
E-mail: dxwang@scsio.ac.cn

The abstract for this article can be found in this issue, following the table of contents.

DOI:10.1175/BAMS-D-14-00159.1

In final form 28 January 2015

(He et al. 2002; Lin et al. 2007; F. Chen et al. 2010; G. Chen et al. 2010, 2011). Mesoscale eddies play an important role in transporting heat, salt, and water volumes that vary significantly on interannual basis in relation to ENSO events (Chen et al. 2012; X. Wang et al. 2012). For example, a mesoscale dipole pattern usually exists off the Vietnam coast from summer to fall, with a cyclonic eddy in the north and an anticyclonic eddy in the south (G. Wang et al. 2006; G. Chen et al. 2010). During an El Niño year, this dipole pattern weakens or even disappears because of the weaker summer monsoon wind (e.g., G. Wang et al. 2006; Yang et al. 2007; Du et al. 2009; Xie et al. 2009), which could lead to an enhanced warm eddy in the northwestern SCS (e.g., Chu et al. 2014). The heat advected by eddies can have a marked effect on the spatial distribution of sea surface temperature (SST) in the SCS, which results in an uneven surface wind field that is faster (slower) over the warm (cold) tongues than the surrounding area (Chow and Liu 2012). This positive correlation between surface wind speed and SST involves synoptic air–sea turbulent momentum and heat transfer in the marine atmospheric boundary layer (MABL).

The SCS warms up rapidly in spring as part of the planetary-scale Indo–western Pacific warm pool (Wang and Wang 2006) but exhibits a pronounced basin-scale cooling during summer, mainly attributed to evaporative cooling by the southwest monsoon wind (Qu 2000; Zhou et al. 2012). Observations have revealed intraseasonal variations of strong upwelling along the south coast of Vietnam and a cold filament that stretches eastward at about 12°N from the coast during June–September each year (Ho et al. 2000; Kuo et al. 2000) in response to the intraseasonal variations of Asian summer monsoon (Xie et al. 2007). The intraseasonal cold filaments tend to reduce the local wind speed and precipitation because of increased static stability in the near-surface atmosphere, indicating the existence of an ocean–atmosphere feedback mechanism (Xie et al. 2007). The intraseasonal cooling of the SST is suppressed in summer following an El Niño event as the southwest monsoon weakens. This process may have contributed to the 1997/98 warm event in the SCS when the SCS throughflow should have been stronger and transported more Pacific water into the SCS through the Luzon Strait (Wang et al. 2002).

Interannual SST anomalies in the SCS are strongly influenced by ENSO events (e.g., Klein et al. 1999; Alexander et al. 2002; Wang et al. 2002). Recent studies have identified a double-peak feature of SST in the SCS following an El Niño event in the Pacific (C. Wang et al. 2006). The first peak is related to positive net heat flux because of the decrease in cloudiness, while the second peak is mainly caused by reduced meridional geostrophic heat advection and thereby weaker cold advection off the Vietnam coast (C. Wang et al. 2006).

As the main moisture source of the SCS summer monsoon, as well as being a region with a high frequency of mesoscale eddies and severe weather systems (e.g., tropical cyclones, storm surges), the SCS imposes a profound impact on the weather and climate change of the surrounding landmass. Thus, there are significant potential benefits to an improved understanding of the regional circulation and air–sea interactions taking place in the SCS. However, progress is hindered by a lack of three-dimensional mesoscale observations of the key dynamic processes in both the atmosphere and ocean in the SCS region.

EARLIER OBSERVATIONS. Observational efforts over the SCS date back to the 1960s, when data were mainly obtained from in situ deep casting during research cruises (C. Liu et al. 2012). Observations during the 1970s relied on a small number of research cruises and focused on the coastal shelf for studies of the Pearl River plume (Ou et al. 2009). A few deep-cast datasets were collected in the northern SCS in the early 1980s (C. Liu et al. 2012). Then, from 1989 to 1999, several cruises took place and yielded larger datasets for the southern SCS (SSCS) (Fang et al. 2002). At that time, there were only a few cruise stations in the central SCS (between 12° and 18°N) and around the dynamically energetic regions (e.g., west of the Luzon Strait and east of the Vietnam coast), where mesoscale eddies are active (G. Chen et al. 2010; Zhuang et al. 2010; Nan et al. 2011). Most of these earlier observations did not include meteorological observations, consisting only of conductivity–temperature–depth (CTD) measurements in the ocean. The SCS Monsoon Experiment (SCSMEX), conducted between 1996 and 2001 with a field phase from 1 May to 3 August 1998, was a major international field experiment set up to study the physical processes involved in the onset, maintenance, and variability of the SCS summer monsoon (Lau et al. 2000). Using the meteorological data obtained during the SCSMEX, it was found that the onset of the SCS summer monsoon in 1998 was closely related to the early development of a twin cyclone to the east of Sri Lanka (Ding and Liu 2001). Furthermore, two intraseasonal modes of 30–60 and 10–20 days significantly influenced the SCS monsoon and its related precipitation pattern (Xu and Zhu 2002). A variety of organized mesoscale convective systems were observed during onset of the SCS monsoon, contributing greatly to heavy rainfall

events. The observational data revealed that there is positive feedback between large-scale circulation and mesoscale convective systems, and warm SST in the SCS strongly influences the onset and intensity of the monsoon (Ding et al. 2004). In addition, significant differences have been found in the MABL and ocean thermal structure as well as the air–sea turbulent flux exchange of the northern and southern SCS (Qu 2000; Wang et al. 2010b). The observations from SCSMEX have also been applied in regional models to improve simulations and short-term forecasts (Liu and Ding 2003; Ren and Qian 2001).

Similar to SCSMEX, a few experiments have been conducted in other ocean basins, with the aim of providing short-term regional observations. For example, the Bay of Bengal Monsoon Experiment (Bhat et al. 2001), the Arabian Sea Monsoon Experiment (Sanjeeva Rao and Sikka 2005), the Joint Air–Sea Monsoon Experiment (Webster et al. 2002), the Surface Ocean Lower Atmosphere Study (Duce and Liss 2002), and the Coupled Boundary Layers and Air–Sea Transfer program (Edson et al. 2007).

Important developments in observations related to large-scale air–sea interactions have taken place in recent decades. For instance, the 8-yr (1990–97) World Ocean Circulation Experiment (Siedler et al. 2001) was a major international effort established to study ocean–atmosphere interactions and basin-scale ocean circulation patterns related to climate. The Global Ocean Observing System (GOOS) is a permanent global system for observations, modeling, and analysis of marine and ocean variables to support operational ocean services worldwide. The Tropical Atmosphere Ocean/Triangle Trans-Ocean Buoy Network (TAO/TRITON; McPhaden et al. 1998; Kuroda and Amitani 2000) provides high-quality moored time series and related data throughout the global tropics for improved description, understanding, and prediction of seasonal to decadal time-scale climate variability, such as ENSO.

OBJECTIVES. In this paper, we describe a mesoscale observation network in the SCS that consists of both oceanic and meteorological observations during cruises and at stations. The network was designed based on the dynamic characteristics of the regional circulation and air–sea interaction over the SCS. The observations were mainly concentrated in dynamically active areas, such as those where coastal upwelling occurs (e.g., the northern SCS, Hainan Island, and coastal Vietnam), where the Kuroshio intrusion via Luzon Strait takes place, and where enhanced eddy activity, continental shelf flow, and mini warm pools are prevalent. The oceanic processes in these key regions represent the main dynamic characteristics of the SCS, and their related air–sea interactions have direct impacts upon the economies and human activities of the surrounding countries. Collecting observations at mesoscale resolution in these key regions (in terms of both horizontal mapping and vertical profiles) is an important approach to investigating regional air–sea coupling in the SCS under current research-funding conditions. Observations in other areas are relatively sparse but will hopefully be enhanced in the future as extra funding becomes available and more national and international collaborations are established. The network was designed to fulfill the following three objectives:

1) To provide vertical profiles of oceanic and atmospheric variables, which can then be used to study the baroclinic structures of the atmospheric and oceanic circulation in the SCS. For example, the variation of the MABL height in the SCS before and after SCS monsoon onset has been well depicted by sounding data (Wang et al. 2010b). The vertical structure of mesoscale eddies can only be captured by in situ measurements (e.g., Nan et al. 2011). Furthermore, in situ observations can also promote the study of the formation of the SCS warm current in the intermediate ocean layer of the northern SCS, which is mainly controlled by baroclinicity combined with topography and is normally referred to as the joint effect of baroclinicity and relief (JEBAR). JEBAR is the dominant forcing of the across-shelf transport in the shelfbreak area (Wang et al. 2010a). The current mainly flows northeastward along the northern SCS continental shelf against the prevailing wind (Xue et al. 2004; Wang et al. 2004; Liao et al. 2007; Yuan et al. 2008; Wang et al. 2013a), possibly resulting in the redistribution of heat content.
2) To provide simultaneous atmospheric and oceanic observations—essential for air–sea coupling studies, particularly on the synoptic time scale. Earlier observations focused mostly on oceanic variables, such as temperature and salinity profiles and ocean currents; very few meteorological observations were made over the SCS at that time. The current network was designed to include both meteorological and oceanic observations during cruises and at stations. Using data from automatic weather stations (AWSs) as well as CTD

and sounding data in the observation network, R. Shi et al. (2014, personal communication) reported a dramatic decrease of the MABL height corresponding to a synchronous fall of SST.

3) To provide data that can be used to evaluate satellite observations and to assess and calibrate model outputs. Errors from satellite-derived products and model results can be validated by comparing them with regional in situ observations (e.g., Qiu et al. 2009; Zeng et al. 2009; Li et al. 2012; Peng et al. 2012; Li et al. 2014). For example, Advanced Very High Resolution Radiometer (AVHRR) SSTs were found to have significant regional biases of about −0.4°C when compared to the drifting buoy SSTs; when the satellite-derived wind speed decreased to below 6 m s^{-1}, the satellite SSTs became higher than the corresponding in situ SSTs (Qiu et al. 2009). If a systematic bias is apparent and there exists a reasonably high spatial–temporal correlation between modeled or satellite-derived variables and in situ–measured variables, independent validation data can be used to remove these systematic biases through statistical regression (Tippett et al. 2005).

REGIONAL HYDROLOGICAL AND MARINE METEOROLOGICAL OBSERVATIONS NETWORK

Establishment and development of the observation network. In 2004, the SCS Institute of Oceanology (SCSIO) conducted a cruise in the northern SCS (18°–23°N, 110°–120°E) during late summer (August–September) (Fig. 1). Along the cruise routes, consecutive oceanic and meteorological observations were made, including SST and sea surface salinity [depth of 5 m; via underway conductivity–temperature (CT)], vertical temperature and salinity profiling [depth of 200 m; via Moving Vessel Profiler (MVP)], current [depth of 500–1000 m; via shipboard acoustic Doppler current profiler (ADCP)], and surface (10 m) meteorological variables (air temperature and pressure, wind, and relative humidity; via AWSs). At each site (markers in Fig. 1), CTD measurements were made to obtain the profile of temperature and salinity (to 1500 m). A mooring is deployed at the east of Vietnam coast. Sensors on the mooring line can measure ocean temperature, conductivity and pressure (at about 10-min intervals), and current profile (at about 1-h intervals). Surface meteorological observations can be used to study the characteristics of MABL. Before 2004, studies on the general characteristics of the MABL in the SCS were limited because of a lack of in situ observations (Wang et al. 2010b). Eight transects (Fig. 1) were carefully designed based on research interests and important scientific issues, including the Pearl River plume (E1 and E7), coastal upwelling (E2 and E6), Taiwan shallow water (E3), circulations around Hainan Island (E4-1 and E5), and Luzon Strait transport (E4-2). Because of its location (18°N) at the boundary of the tropics and subtropics, transect E4-1 was a regular transect of the Climate and Ocean: Variability, Predictability and Change (CLIVAR) program, designed to study meridional ocean transport, atmospheric meridional circulation, and monsoon activity. The cruise was an open cruise that welcomed other research units on board to carry out their own experiments. A total of nine research institutions, including three universities and six institutes participated in the 2004 SCSIO open cruise. Later as an annual event, the SCSIO open cruise surveys approximately the same area during the same season each year.

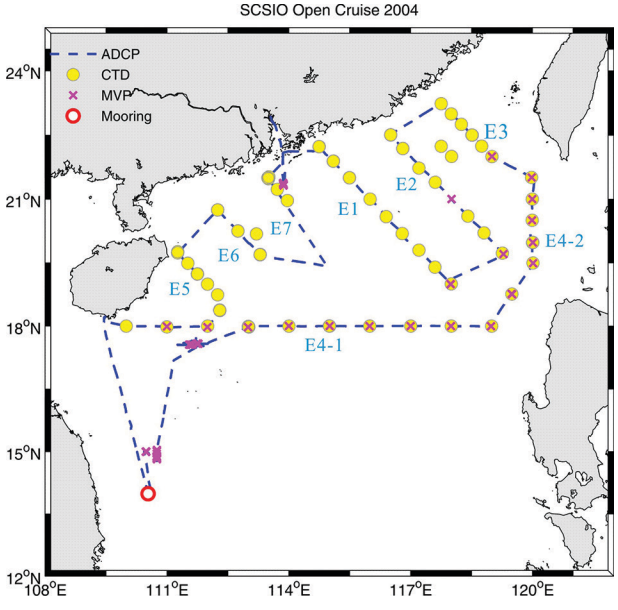

Fig. 1. Cruise tracks in the SCS during the 2004 SCSIO open cruise (the labels E1–E7 indicate the cruise transects).

Since 2006, the SCSIO open cruise has carried a radiometer and conducted global positioning system (GPS) soundings, marking a new era of marine meteorological observation in the SCS. The sounding balloon is an excellent way to obtain the vertical temperature and humidity structure of the atmosphere over the ocean (Wang et al. 2010b). GPS sounding balloons are launched regularly during each cruise to obtain vertical profiles of wind, air temperature, and humidity. Figure 2 shows an example of the measurements obtained from GPS sounding as well as a picture of cruise members releasing a sounding balloon. Measurements can vary with different

choices of radiosonde. Two radiosondes—GPS-TK radiosonde, manufactured by the Key Laboratory of Middle Atmosphere and Global Environment Observation of the Institute of Atmospheric Physics, Chinese Academy of Sciences (CAS), China, and the CF-06-A radiosonde, manufactured by Beijing Chang Feng Microelectronics Technology Co. Ltd., China—are used in the network. Chinese-manufactured radiosondes were preferred because despite the known quality of Vaisala radiosonde, they are very expensive. Nevertheless, radiosonde intercomparisons involving the two types of radiosondes used on the cruises and Vaisala radiosondes suggest that CF-06-A radiosonde performs excellently over the tropical ocean (Nash et al. 2011; Xie et al. 2014). The AWS is now fully equipped with meteorological sensors measuring net radiation, air temperature and pressure, wind direction and speed, and humidity (Fig. 2c).

Besides open cruises, SCSIO has expanded the network by conducting cruises over different areas of the SCS for specific scientific issues. For example, the so-called Xisha cruises were conducted to study the warm eddies near the Xisha Islands, and the southern SCS cruises were conducted to study the mini warm pool—a large area of warm water with a mixed-layer temperature of greater than 29°C (Wang and Wang 2006). Since 2010, the National Natural Science Foundation of China (NSFC) has organized several open cruises in the SCS, allowing scientists to apply for ship time and perform their own experiments on board. Researchers at SCSIO have participated in cruises organized by other research units, such as Xiamen University and the First Institute of Oceanography of the State Oceanic Administration (SOA), among others.

Fixed multifunction observation platforms in the ocean complement cruise observations by providing long-term and continuous real-time data. Observation platforms including buoy, deep-ocean mooring, and meteorological measurements have been set up off the Xisha Islands, Nansha Islands, and along the Luzon Strait. The meteorological measurements on buoys include air temperature, relative humidity, wind velocity, and shortwave radiation. Furthermore, SST and conductivity are measured from the buoys at depths of less than 3 m. Xisha station (constructed in 2007 and operational since 2008) was the first deep-sea observation station to be established in Chinese waters. It is located off the coast of Yongxing Island, one of the main islands of the Xisha group, and is situated in the deep-water (>1000 m) basin of the north-central SCS, about 180 nautical miles (333 km) southeast of Hainan Island. Therefore, Xisha station can be categorized as

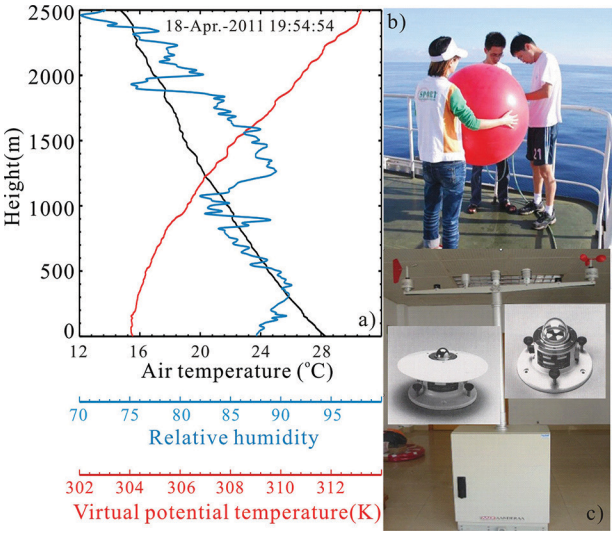

Fig. 2. (a) An example of air temperature, relative humidity, and virtual potential temperature measurements obtained from GPS sounding balloons. (b) Cruise members launching a sounding balloon. (c) The shipboard AWS used during cruises, superimposed by longwave and shortwave radiometers.

both a coastal and a deep-sea station and is equipped with an AWS, moorings, shore-based wave and tide gauges, bottom-moored sediment traps, and moored buoys. Figure 3 shows an example of ADCP measurements as well as a picture of cruise members launching the ACDP into the water. Moorings were deployed (Fig. 3e) in the water near the Xisha site (16.85°N, 112.31°E), and the AWS was installed on the roof of the station building (Fig. 3d). Figure 3c shows that the passages of tropical cyclones and cold surges around Xisha station can be captured well by the data from the AWS and buoys. The 20-m Xisha Island air–sea boundary flux tower located 97 m offshore of Yongxing Island (16.84°N, 112.33°E) has been in operation since 2013. The tower is equipped with gradient and eddy covariance observations for the measurement of air–sea boundary fluxes [Fig. 4a; further details about the flux tower can be found in Shi et al. (2015)]. Figures 4b–d present examples of measurements (1-h moving average) from the tower. Following the methods recommended by a global network of micrometeorological tower sites [flux network (FLUXNET); http://fluxnet.ornl.gov], quality-control measures are routinely applied to the raw data. Since 2011, two high-frequency radar stations have been built by SCSIO at Bohe, Maoming (21.44°N, 111.39°E), and Zhanjiang (20.88°N, 110.12°E), Guangdong Province. Observations from these radar stations can be used to study coastal upwelling/downwelling, fronts, waves, and surface wind. More high-frequency radar stations

will be added along the southern China coastline in the future.

The marine meteorological observation network in the SCS was first brought to a higher level, in terms of both quality and quantity, by the initiation of the Monsoon Asian Hydro-Atmosphere Scientific Research and Prediction Initiative (MAHASRI 2006–15; http://mahasri.cr.chiba-u.ac.jp) and the Asian Monsoon Years (AMY 2007–12; www.wcrp-amy.org/). MAHASRI is one of the regional hydroclimate projects under the Global Energy and Water Cycle Experiment hydroclimatology panel to study the water and energy cycle of the Asian monsoon region and to establish a hydrometeorological prediction system, particularly up to the seasonal time scale. AMY, meanwhile, was a coordinated observational and modeling effort geared toward understanding the radiation–monsoon–water cycle interaction and ocean–land–atmosphere interaction of the Asian monsoon system, as well as improving monsoon prediction. The coordination of these various national projects has facilitated mutual data exchange and new scientific findings, which have led to a deeper understanding of the Asian monsoon, including regional air–sea interaction. MAHASRI collaborated closely with AMY in investigating precipitation systems (Liu et al. 2011; Wu et al. 2011), convection patterns (Fujita et al. 2011), the structure of the MABL and surface fluxes (Ma et al. 2011), and large-scale circulation and air–sea coupling (Lestari et al. 2011) in the Asian monsoon region. The studies were conducted on time scales ranging from diurnal to interannual, mainly using in situ and satellite observations and model simulations.

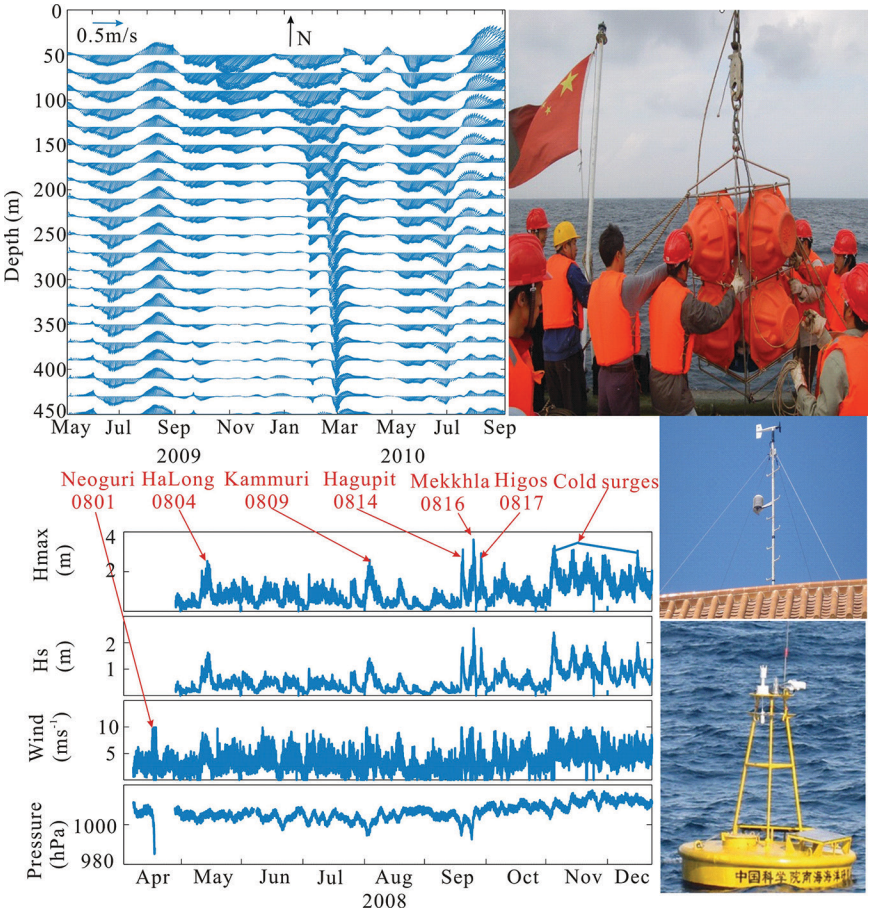

Fig. 3. (a) ADCP measurements at Xisha station during the period from May 2009 to Sep 2010. (b) Cruise members deploying the ADCP. (c) AWS and buoy data (tropical cyclones and cold surges are reflected well in the data, indicated by red arrows and texts. Hs denotes significant wave height; Hmax denotes maximum wave height). (d) The AWS station installed on the roof of the building at Xisha station. (e) Mooring buoy deployed in the waters around Xisha station.

Additional observations have joined the network with the initiation of a key project in China entitled "Air–sea interaction and ocean circulation and eddy evolutions." This project aims to improve understanding of air–sea interaction processes in the SCS through intensive observations, especially air–sea coupling under different weather conditions, the evolution of upper-ocean circulation, and eddies and their thermodynamic and dynamic effects on air–sea interactions and feedbacks of the upper-ocean heat structure to weather systems in the SCS. To achieve these goals, observations have been made in the Luzon Strait, northern SCS continental shelf, coastal Vietnam, and the southern SCS.

Multi-institution collaboration. Besides the cruises and stations mentioned in the section titled "Establishment and development of the observation network," the SCSIO has also been an active participant in, or coorganized, several cruises conducted by other institutes. For instance, the northern SCS Coastal

Oceanographic Process Experiment Pilot Project (SCOPE-PP) cruise was jointly organized by five institutes in China in 2008 for studying the upwelling off the east Guangdong coast and related environmental impacts. Other cruises have included the Main Program of Knowledge Innovation of the Chinese Academy of Sciences (MPKI) cruise, the Response of Marine Hazards to Climate Change in the Western Pacific (ROSE) cruise, and the State Key Laboratory of Marine Environmental Science of Xiamen University (MEL) cruise. Further details about these cruises are provided in Table 1. Furthermore, a mooring array including five mooring buoys from SCSIO and the First Institute of Oceanography of the SOA will be deployed next year off the southeast coast of Hainan Island for thorough investigations of the western boundary current.

The Marine Meteorological Science Experiment Base (MMSEB) at Bohe was jointly established in 2006 by Guangzhou Institute of Tropical and Marine Meteorology (GITMM) and Maoming Meteorological Bureau (MMB) under the Guangdong Meteorological Service (GMS) of the China Meteorological Administration (Fig. 5). This base is dedicated to the construction of a marine meteorology observation network over the coastal areas of southern China. The MMSEB is mainly composed of Beishan station, an integrated observation platform, and a 100-m observation tower. Beishan station is used to measure the vertical structure of the atmospheric boundary layer, meteorological elements near the surface, and variables related to the marine environment. The integrated observation platform is situated at a distance of 6.5 km from the coast (Figs. 5a,c) and was designed to observe the processes related to the atmospheric and oceanic boundary layers and their interactions. The 100-m observation tower is located on an island about 5 km from the coast (Figs. 5a,d) and is used to measure air–sea boundary fluxes and wind energy. Comparison of wind direction measurements between radar wind profiler and GPS sounding indicates a general consistency between the two instruments (Fig. 5e). All the data from the base are subject to quality-control measures following the recommendations of FLUXNET (Fig. 5f). The MMSEB was established mainly for operational purposes; however, it is also an open station for scientific research activities. For example, the radar station at Maoming, established by the SCSIO, was built inside the MMSEB. In addition, three buoys off the coast of the cities of Maoming, Shantou, and Shanwei and three oil platform–based AWSs (Panyu, Liuhua, and Lufeng) established by the GMS in 2006 have also been included in the network (Fig. 6; Table 1). Further details about MMSEB can be found in Huang and Chan (2011), and details of the abovementioned stations are presented in Table 2. Note that some cruises and stations from other research units not included in the network are not listed because their data have not been released to the public.

With the various multi-institution collaborations that took place during 2004–13, the observation

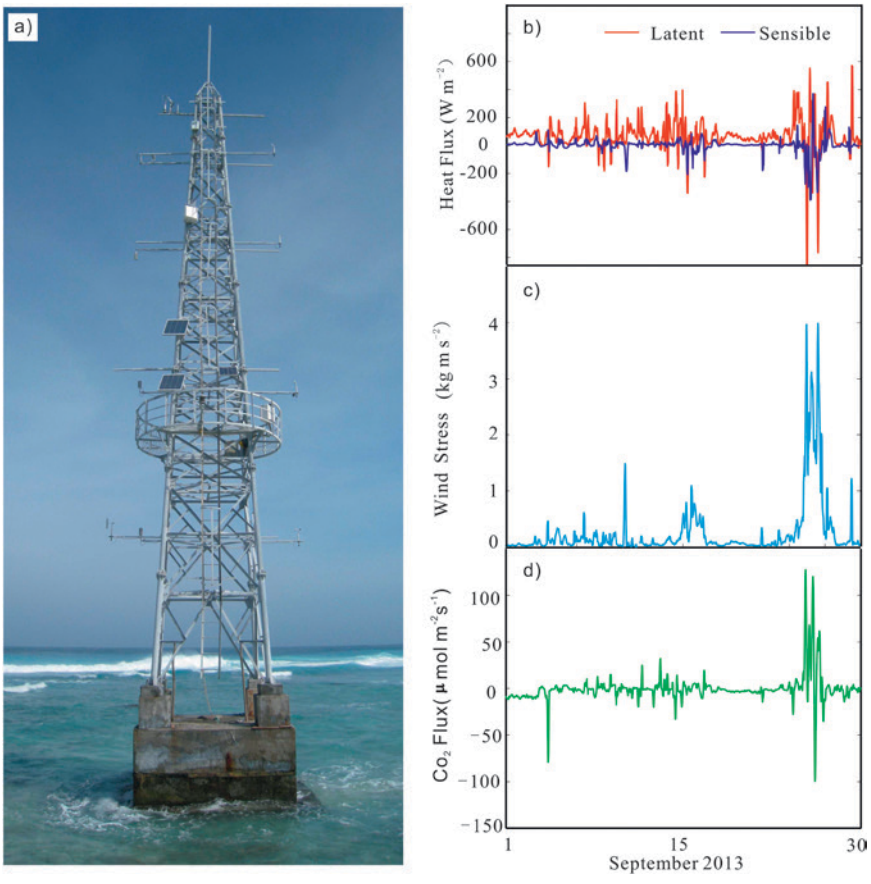

Fig. 4. (a) The Xisha flux tower and three examples of measurements (1-h moving average): (b) latent and sensible heat fluxes, (c) wind stress, and (d) CO_2 fluxes.

Table 1. List of cruises in the network.

Station or cruise	Lat (°N)	Lon (°E)	Deployment period	Organized by
Open cruise 2004	14.39°–22.19°	109.48°–119.45°	17 Sep–4 Oct 2004	SCSIO
Open cruise 2005	13.38°–22.24°	109.48°–119.61°	5–22 Sep 2005	SCSIO
Open cruise 2006	17.98°–22.25°	109.47°–120.01°	9–28 Sep 2006	SCSIO
MEL cruise 2006	10.50°–22.15°	110.20°–119.00°	26 Nov–16 Dec 2006	Xiamen University
SSCS cruise 2007	5.38°–20.87°	108.49°–117.98°	15 May–20 Jun 2007	SCSIO
Open cruise 2007	17.95°–23.39°	110.06°–120.03°	13–27 Aug 2007	SCSIO
Cruise 200709	18.01°–25.01°	111.13°–119.75°	24–29 Sep 2007	SCSIO
Cruise 200803	18.89°–22.70°	112.64°–113.85°	16–20 Mar 2008	SCSIO
SCOPE-PP cruise 2008	20.27°–23.53°	114.07°–117.96°	29 Jun–14 Jul 2008	Five institutes*
Open cruise 2008	17.01°–22.41°	109.50°–119.98°	16 Aug–4 Sep 2008	SCSIO
SSCS cruise 2009	6°–18°	108°–119.5°	28 Apr–20 Jun 2009	SCSIO
MPKI cruise 2009	18.21°–33.72°	109.49°–122.55°	9 Jun–5 Jul 2009	Institute of Oceanography of the CAS
ROSE cruise 2009	9.19°–19.55°	110.31°–117.96°	19 Jun–30 Jun 2009	First Institute of Oceanography of the SOA
Open cruise 2009	15.77°–22.57°	109.55°–120.09°	1–19 Sep 2009	SCSIO
NSFC cruise 2010	8°–23°	110°–120°	24 Apr–25 May 2010	SCSIO
Xisha cruise 2010	16.5°–19°	110.5°–113.2°	10–14 Aug 2010	SCSIO
Open cruise 2010	18°–22°	110°–120°	31 Aug–23 Sep 2010	SCSIO
Open cruise 2010	16.93°–23.05°	110.30°–120.01°	2–20 Sep 2010	SCSIO
ROSE cruise 2010	7.06°–19.00°	109.95°–117.95°	26 Oct–11 Nov 2010	First Institute of Oceanography of the SOA
SSCS cruise 2010	6°–18°	108°–120.11°	27 Oct–20 Nov 2010	SCSIO
Xisha cruise 2011	16.47°–18.39°	109.56°–111.74°	2–5 Jun 2011	SCSIO
Open cruise 2011	16.97°–22.32°	109.44°–120.02°	21 Aug–10 Sep 2011	SCSIO
SSCS cruise 2011	6°–18°	105.5°–114°	28 Nov 2011–12 Jan 2012	SCSIO
Xisha cruise 2012	15.64°–17.74°	110.04°–112.33°	15–25 May 2012	SCSIO
SSCS cruise 2012	6°–22°	108°–119°	6 Aug–12 Sep 2012	SCSIO
NSFC open cruise 2012	14°–22°	110°–119°	26 Sep–29 Oct 2010	SCSIO
Open cruise 2012	17.27°–21.93°	108.49°–113.74°	13–22 Dec 2012	SCSIO
Xisha cruise 2013	14.96°–18.41°	110.79°–116.54°	14–26 Aug 2013	SCSIO
NSFC open cruise 2013	9.8°–21.3°	110.3°–114°	5 Aug–6 Sep 2013	SCSIO
NSFC open cruise 2013	14.1°–23°	110.3°–118°	24 Sep–24 Oct 2013	SCSIO

* Xiamen University, the SCSIO, the Institute of Atmospheric Physics (CAS), the Third Institute of Oceanography of the SOA, and the Hong Kong University of Science and Technology.

network has archived data from seven buoys, three stations, and three platforms, as well as a total of 30 cruises in the SCS, including 10 SCSIO open cruises in the northern SCS, 4 Xisha cruises, 5 southern SCS cruises, 4 NSFC open cruises, and 7 other cruises (Tables 1 and 2; Fig. 6). These cruises, together with the Xisha, Nansha, and MMSEB stations, radar stations, and moorings (Table 2), have formed an extensive observational network, covering the entire SCS and its vertical extent from sea floor to approximately 20 km above the sea surface (Fig. 6). Regular cruises (with surveying frequencies) and stations are displayed in Fig. 7. The minimum distance between cruise stations is approximately 20 km, which is within the Rossby radius of deformation of both the ocean (~20–120 km; Cai et al. 2008) and atmosphere (10–200 km, with the time scale from hours to days for mesoscale processes; Fujita 1981). Subsequently, the observations from these cruises and fixed stations have been capable of resolving mesoscale processes, such as eddies (Nan

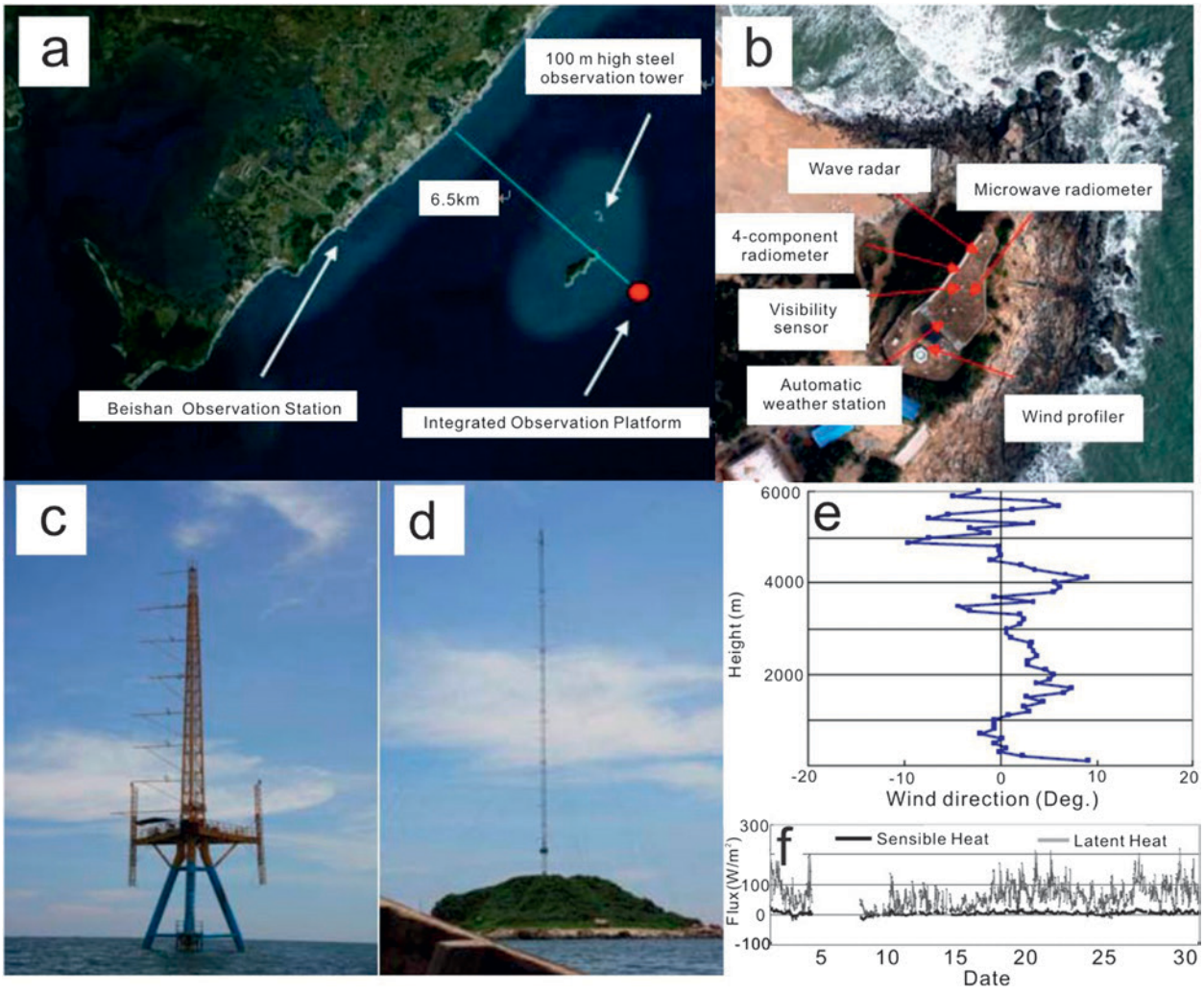

Fig. 5. The major facilities and experiments of the MMSEB: (a) distribution of the observation facilities, (b) Beishan station, (c) integrated observation platform, (d) 100-m-high observation tower, (e) the mean difference of wind direction between wind profiler and GPS radiosonde, and (f) the sensible and latent heat fluxes after quality control.

et al. 2011; He et al. 2013), fronts (Shi et al. 2014), and coastal upwelling (Wang et al. 2013a) in the ocean, as well as synoptic weather processes such as cold surges and tropical cyclones in the atmosphere. For example, Li et al. (2006) investigated the impact of cold surge on SST and air–sea heat fluxes. Two cold surges occurred in the northern SCS during the 2004 open cruise, which were captured well by the observations. It was found that the first surge (21–22 September) was very weak and did not pose any significant impact on SST. However, the faster and stronger surge that occurred on 2 October caused a significant drop in SST in the SCS.

SCIENTIFIC APPLICATIONS. As part of a multi-institute collaboration, a mesoscale hydrological and marine meteorological observation network is being developed, and the data collected have been subsequently utilized in a variety of research areas related to the investigation of air–sea interaction.

Regional circulation in the SCS since the 1990s. The circulation of the SCS is controlled by monsoons, complicated topography, and water exchange in its straits. In the intermediate ocean layer, JEBAR play an important role in the formation of the SCS warm current, which mainly flows northeastward over the northern SCS continental shelf and has potential impacts on regional atmospheric circulation (Wang et al. 2004, 2013; Liao et al. 2007; Yuan et al. 2008). The SCS warm current consists of two distinct parts. The eastern part exits east of the Dongsha Islands and flows steadily northeastward, while the western part is located west of the Dongsha Islands (Guan 1985). The eastern part is stronger, wider, and deeper than the western part. The eastern part of the SCS warm

Table 2. List of stations in the network.

Station or cruise		Lat (°N)	Lon (°E)	Deployment since	Deployed by
Buoys and stations	Sanya Bay buoy	18.21	109.45	2009	SCSIO
	Shanwei buoy	22.60	115.55	9 Jan 2010	GMS
	Maoming buoy	20.73	111.65	27 Mar 2011	GMS
	Shantou buoy	22.31	117.33	27 Mar 2011	GMS
	Xisha mooring buoy	17.1	110.38	Aug 2007	SCSIO
	Nansha mooring buoy	9.78	112.93	Aug 2007	SCSIO
	Luzon mooring buoy	20.55	119.86	Aug 2007	SCSIO
Observation stations (including AWSs, flux tower, and platforms)	Xisha station	16.83	112.33	6 Apr 2008	SCSIO
	Nansha station	9.78	112.93	6 Apr 2008	SCSIO
	Liuhua platform	20.82	115.7	26 Dec 2006	GMS
	Panyu platform	20.23	114.93	16 Nov 2010	GMS
	LeFeng platform	21.58	116.15	5 Dec 2010	GMS
	MMSEB station	21.46	111.32	2006	GITMM and MMB under GMS

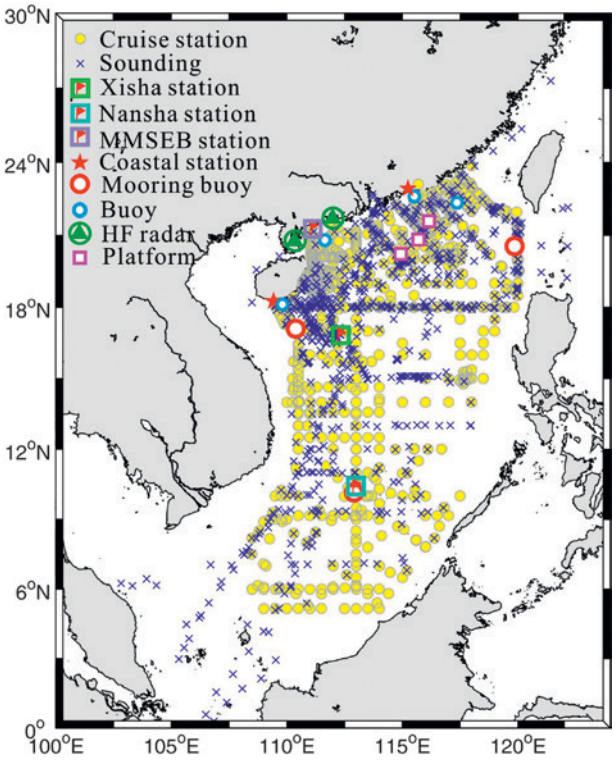

Fig. 6. Locations of the measurements in the observation network during the period 2004–13.

current flows eastward along the isobath, and then veers off toward the deep sea while it flows around the Dongsha Islands (Liao et al. 2008). ADCP and CTD data during the 2005 SCSIO open cruise confirmed the deflection. It was found that baroclinicity and topography are mainly responsible for the deflection. The along-isobath gradient of the density field interacts with the topography that supplies negative potential vorticity and drives the column-integrated flow away from the isobaths, veering toward the deep sea (Wang et al. 2013a).

In summer, under southwesterly monsoon forcing, a northeastward current, denoted as the western boundary current of the SCS, flows along the Vietnam coast, the south and east coasts of Hainan Island, and the northern SCS coast (Su 2004). Upwelling usually occurs along these coasts because of the wind and topographical effects (e.g., Xie et al. 2007; Jing et al. 2009; Su and Pohlmann 2009; Shu et al. 2011a; X. Zeng et al. 2014). Cold-water spread related to upwelling can reduce the local wind speed and precipitation because of the increased static stability in the near-surface atmosphere, indicating the existence of an ocean–atmosphere feedback mechanism (Xie et al. 2007). Under the influence of the upwelling-favoring wind and coastal jet in the northern SCS, the Pearl River plume spreads mainly eastward and plays an important role in regional air–sea coupling and chemical and/or biological transport processes (Wyrtki 1961; Guan and Chen 1964; Xue et al. 2001; Gan et al. 2009; Jing et al. 2009; Zu and Gan 2015). By assimilating CTD measurements obtained from SCOPE-PP (2008) into a regional ocean model, the three-dimensional structure of the upwelling and Pearl River plume was obtained (Shu et al. 2011b). It was found that the mechanism of upwelling in the northern SCS is directly related to the topography and large-scale currents in addition to the local wind (Shu

et al. 2011a). Topography-induced upwelling was also observed in the northern SCS using observations from four SCSIO open cruises when the upwelling-favoring wind retreated (Wang et al. 2014).

The SCS basin is characterized by seasonally varying precipitation (Xie et al. 2003), strong river discharge (Ou et al. 2009), and intrusion of high-salinity water from the Kuroshio through the Luzon Strait (Dale 1956; Wyrtki 1961; Nan et al. 2013). The salinity in the SCS also exhibits pronounced variability on different time scales. Nan et al. (2013) noted that the upper ocean has become less saline in the northern SCS over the past two decades. L. Zeng et al. (2014) identified a freshening of up to 0.4 psu in the upper ocean of the northern SCS in 2012 using satellite observations, which were evaluated against in situ observations from the SCS observation network and Argo floats during 2011–13. The study suggested that the freshening in 2012 might have been caused by the combined effect of abundant local freshwater flux and limited Kuroshio intrusion.

High mesoscale eddy activity and unique regional air–sea coupling patterns have been observed in the SCS (Dale 1956; Qu 2000; Chu and Fan 2001; G. Wang et al. 2006; Yuan et al. 2007; Chen et al. 2009, 2011; He et al. 2013; Chu et al. 2014). The geographic distribution of eddy energy shows that the higher eddy kinetic energies are located to the east of Vietnam and to the west of Taiwan (Chen et al. 2009; Cheng and Qi 2010). Although eddies and their evolutions can be tracked and depicted using satellite sea surface height anomaly data, their vertical structures, such as vertical profile of temperature, salinity, density, and velocity, cannot be analyzed without in situ hydrographic data. In August 2007, three anticyclonic eddies moved across E4-1 during the observational period of that year's SCSIO open cruise. The CTD and ADCP data, as well as those from drifting buoys, successfully captured the vertical structure of the three eddies and their evolutions (Nan et al. 2011). The CTD-measured temperature/salinity profiles established during several cruises were used to confirm the existence of a recurring spring mesoscale eddy with a warm core and low salinity, named the spring mesoscale high (SMH) in the western SCS (He et al. 2013). The climatological SMH first appears east of the central Vietnam coast in February as a high sea level anomaly, grows rapidly to a well-developed anticyclonic eddy by March, matures in April, and decays in May each year. It was found that the SMH always emerges in the region (12°–16°N, 110°–114°E), although with clear interannual variations in terms of intensity and size. The formation of the SMH is

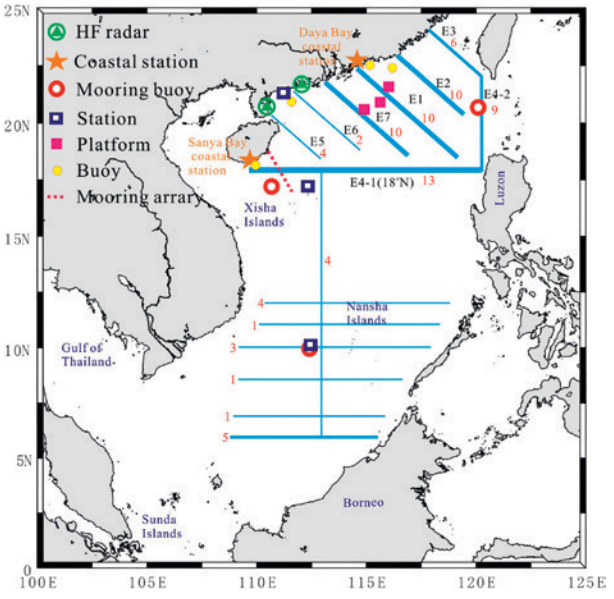

Fig. 7. Schematic diagram of the observation network's regular cruises and stations (including ground wave radars, coastal stations, and mooring buoys) in the SCS. Blue lines represent the cruise transects. The labels E1–E7 indicate the cruise transects for the northern SCS open cruises. Red numbers alongside each cruise transect denote the frequency during 2004–13. The red dashed line represents the location of a mooring array, which is still under construction.

attributed to both wind forcing and the release of potential energy by the winter monsoon (He et al. 2013). In 2010, an extremely large and long-lasting warm eddy was observed in the SCS to be moving northward from the south of the Xisha Islands. The CTD and expendable bathythermographs measurements obtained during the 2010 warm eddy cruise were used to explore the eddy's vertical structure (Chu et al. 2014). A seasonal eddy dipole pattern usually exists off the Vietnam coast from summer to fall, with a cyclonic eddy in the north and an anticyclonic eddy in the south (G. Wang et al. 2006; G. Chen et al. 2010). However, a strong El Niño event in 2009/10 altered the intensity and direction of the summer monsoon, resulting in the disappearance of this pattern and the northward movement of a preexisting warm eddy along the Vietnam coast. During this northward movement, the western boundary current cascaded energy to the eddy, which led to its continuing growth in both strength and size. The CTD data obtained during the 2007 SCSIO open cruise were used to explore mesoscale eddy-induced transport features in the northern SCS. Relatively large poleward eddy heat transports occurred east of Vietnam in summer and west of the Luzon Islands in winter, while

a large equatorward heat transport was located west of the Luzon Strait in winter (Chen et al. 2012). Such intensified eddy transports are mostly related to the combined effect of vertical velocity shear, latitude, and stratification determined by the intensity of baroclinic instability.

In the past three decades, high-resolution SST data have been obtained through satellite remote sensing. There are two kinds of sensors involved in producing these data: infrared sensors and microwave sensors. Infrared sensors are affected by clouds and aerosols (Guan and Kawamura 2004), while microwave sensors are influenced by wind speed, columnar water vapor, cloud water content, and rain rate (e.g., Wentz et al. 2000). Using observations from the SCSIO open cruises, Qiu et al. (2009) found that AVHRR SSTs had significant regional biases of about −0.4°C when compared with drifting buoy SSTs; when the satellite-derived wind speed decreased to below 6 m s^{-1}, the satellite SSTs became higher than the corresponding in situ SSTs. Validation of Moderate Resolution Imaging Spectroradiometer (MODIS) SST over the SCS has also been made using in situ data from Xisha station and SCSIO cruises during 2008–12 (Qin et al. 2014). The study revealed that MODIS SST had a bias ranging from −0.35° to −0.19°C and a root-mean-square error of about 0.7°C. Relatively large errors at night indicated the possibility of cloud contamination of the MODIS SST dataset (Qin et al. 2014).

Processes in the MABL. SST perturbations associated with eddies, oceanic fronts, and other oceanic processes can induce adjustment of the MABL and result in perturbations of surface wind, with enhanced winds over warm water and reduced winds over cold water (e.g., Koblinsky et al. 1984; Small et al. 2008; Chow and Liu 2012). Based on GPS sounding data from the SCSIO open cruises, Shi et al. (2014) revealed a thicker (thinner) MABL over the warm (cold) SST side of a coastal front. The MABL is the part of the atmosphere that has direct contact with the ocean and hence interacts directly with it. Thus, the MABL is where the ocean and atmosphere exchange heat, moisture, and momentum, primarily via turbulent fluxes (Fairall et al. 1996). Air–sea boundary fluxes vary with meteorological conditions, such as monsoon onset and retreat and sea fog. Using data from the Xisha flux tower, it was found that both boundary momentum and heat flux exchanges responded strongly to the retreat of the monsoon around 7 September 2013 (Shi et al. 2015). In another study, the boundary heat flux data obtained at the MMSEB flux tower showed that, in the formation and dissipation stages of a sea fog event during 24–25 March 2007, the heat flux was rather small and the fog layer was mainly determined by the mechanical turbulence associated with wind shear; however, in the development and persistence stages, the heat transport near the sea surface increased as a result of longwave radiative cooling near the fog top, and the vertical extension of the fog layer occurred at about the same time as the increase in heat flux (Huang and Chan 2011). Boundary momentum flux and basic oceanic and atmospheric variables, such as wind, precipitation, SST, and salinity, can also be obtained directly by satellite observation, while surface radiation fluxes and sensible and latent heat fluxes can be determined using a radiation transfer model and bulk turbulent flux model using satellite-derived variables (Curry et al. 2004). A high-resolution daily latent heat flux product for the SCS was developed based on data from satellite measurements along with in situ observations (Zeng et al. 2009). Much earlier, near-surface specific humidity was computed using the global relationship based on satellite percipitable water (Liu 1986). In a more recent study, Wang et al. (2014) further verified satellite-derived air specific humidity against 1,016 high-resolution radiosonde profiles during 1998–2012 and the time series from the AWS at Xisha during 2008–10. Compared with five other global latent heat flux products, the daily latent heat flux product in the SCS shows the highest spatial resolution and realistic magnitude for the region. In the lower MABL, atmospheric ducts frequently occur, which can result in nonstandard electromagnetic propagation of radar signals and wireless communications. An effective method for detecting atmospheric ducts is to use radiosonde to measure the height dependence of temperature, pressure, and humidity (Mentes and Kaymaz 2007). GPS sounding data from the SCSIO open cruises were used to study the characteristics of atmospheric ducts over the SCS. The results showed that the occurrence probabilities of evaporation ducts, surface-based ducts, and elevated ducts were 75.3%, 5%, and 43.7%, respectively, and the mean evaporation duct height was 15.3 m (Zhao et al. 2013).

Atmospheric disturbance and tropical cyclones. Disturbances in the tropical atmosphere play important roles in the dynamics of global climate. Typically, disturbances in the tropical atmosphere are induced by waves propagating over different periods and in different directions. These waves, especially the easterly waves, are associated with organized convection and have great influence on precipitation. Based on observational data from the AWS at Xisha and three moorings in the continental shelf region of the

northern SCS, Zeng et al. (2012) found that synoptic perturbations are most active in August, and their interannual variability bears a close relationship with El Niño. Two active phases appear after an El Niño: one in the El Niño mature phase and the other in the summer of the El Niño decay year.

There is strong tropical cyclone activity in the SCS, and it demonstrates significant seasonal, interannual, and interdecadal variation (e.g., Wang and Fei 1987; Chan 1995; Chan and Xu 2009; Wu et al. 2010; Yang et al. 2012, 2015). Regular cruises often try to avoid such disastrous weather for obvious safety reasons. Therefore, in situ data for studies of extreme marine meteorological conditions mostly derive from observations made at fixed stations and buoys. A total of 52 tropical cyclones passed over the SCS during the period 2008–2011, and 21 of those 52 were found to be less than 400 km away the Xisha station (D. Wang et al. 2012). Using the AWS and buoy data from Xisha station, studies have shown that atmospheric variables and air–sea interaction during tropical cyclone passages experience significant changes (Long et al. 2010; D. Wang et al. 2012).

DATA MANAGEMENT, END USERS, AND OUTREACH. A lack of professional technical teams is a major obstacle to the continued rapid development of the mesoscale network in the SCS. Without professional technicians, it is difficult to provide reliable and efficient technical solutions, program implementation, equipment operation and maintenance, sample analysis, data management (including quality control), and other technical support. In the future, it is hoped that training workshops will be regularly organized for both cruise members and data management personnel to ensure the quality of raw data. As the data in the observation network continue to grow, management of the rapidly increasing number of diverse datasets and the associated metadata is a recognized concern. It is necessary to construct a set of management procedures, including network expansion design, sensor installation and calibration, data collection, point measurement upscaling, data quality control, and data archiving. Data collected during each cruise are stored into our data server at the end of the cruise, and measurements from fixed station are transferred back to the server in real time. All data are subject to careful quality control through checking each time series one by one, such that unrealistic or inaccurate data can be flagged. The data of individual cruise can be accessed through the data archive website (http://ocean.data.ac.cn/) by submitting an application to each dataset (Xu et al. 2010; Huo et al. 2012). An introduction to each of the instruments used in the observation network can be found at the open cruise website of the SCSIO (http://lto.scsio.ac.cn).

The observational data from the network can be used for both research and real-time environmental monitoring. To date, the observation datasets along the western boundary have formed a clear monitoring network for the coastal area of southern China (Fig. 8). Data from the observation network can also be applied in ecosystem research (Zhao et al. 2009; X. Liu et al. 2012). The International Workshop on Marine Environment Change has been successfully organized by the SCSIO every 2 years since 2001, and studies related to the marine ecosystem presented in

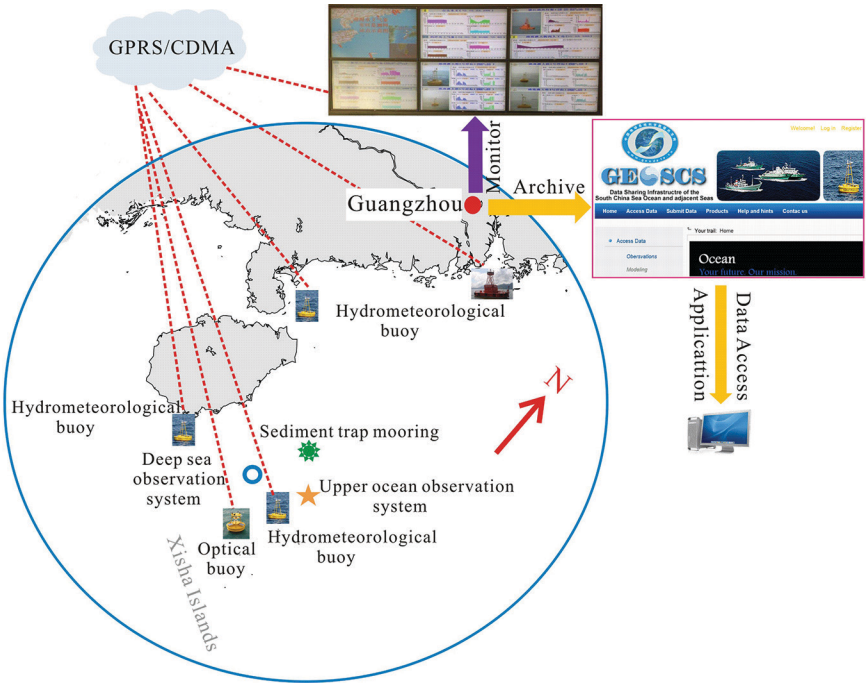

Fig. 8. The observation network to benefit marine environmental monitoring in the coastal area of southern China (GPRS: General Packet Radio Service; CDMA: Code Division Multiple Access).

the fifth workshops were published in the special issue of *Aquatic Ecosystem Health and Management* (2012, Vol. 15, No. 1). Most of the papers published in the issues utilized the in situ observations of the network in the SCS. Their dissemination has enhanced scientific exchange on atmospheric and oceanic dynamics and ecosystem research in the SCS, attracting worldwide attention to the field and promoting future collaboration.

Observations from the network could also contribute to those international research communities interested in constructing global or larger-scale datasets using upscaling techniques, as was the case with AMY. To encourage the use of the network's data by the broader community, we also cooperated with AMY in publicizing the dataset. Both national and international efforts should be pooled to develop a three-dimensional and fully functional observation network in the SCS. In the future, advanced observational instruments should be adopted in the observation network. Mooring arrays have been widely used in global and regional observation networks because of their capability in providing long-term, continuous time series of data at high resolution. The future development of the observation network should include a subnetwork of mooring arrays, similar to those in other ocean basins, such as TAO/TRITON, the Research Moored Array for African–Asian–Australian Monsoon Analysis and Prediction (RAMA; McPhaden et al. 2009), the Prediction and Research Moored Array in the Tropical Atlantic (PIRATA; Bourlès et al. 2008), the Baltic Operational Oceanographic System (BOOS; Dahlin 1997), and Mediterranean Oceanography Network for the Global Ocean Observing System (MONGOOS; www.mongoos.eu/). Gliders are autonomous vehicles that profile vertically by controlling buoyancy and move horizontally on wings, which are very efficient for taking measurements over long periods using a range of sensors (Rudnick et al. 2004). Data obtained from gliders were successfully used to reveal the importance of atmospheric teleconnections in the California Current System during the 2009/10 El Niño, which, if carried out using ship-based observation, would have required great expense and substantial manpower (Todd et al. 2011). In the future, an extensive mooring array and gliders will be applied in the observation network to achieve long-term, sustained observations with fine spatial and temporal resolutions.

ACKNOWLEDGMENTS. The authors would like to thank three anonymous reviewers and BAMS subject matter editor Dr. Michael McPhaden for helpful comments on earlier versions of this manuscript. This work was supported by the National Basic Research Program "973" Program of China (2011CB403500 and 2011CB403504), the Strategic Priority Research Programs of the Chinese Academy of Sciences (CAS) (XDA11010302, XDA11010403) the CAS/SAFEA International Partnership Program for Creative Research Teams, and the National Natural Science Foundation of China (41476014, 41206011, 41422601, 41306012, 41306014, 41106028). We thank Dr. Gengxin Chen and Dr. Yeqiang Shu for the useful discussions and thank Mr. Danian Liu, Mr. Ke Huang, and Mr. Jingen Xiao for their help with data collection.

REFERENCES

Alexander, M. A., I. Bladé, M. Newman, J. R. Lanzante, N.-C. Lau, and J. D. Scott, 2002: The atmospheric bridge: The influence of ENSO teleconnections on air–sea interaction over the global oceans. *J. Climate,* **15,** 2205–2231, doi:10.1175/1520-0442(2002)015<2205:TABTIO>2.0.CO;2.

Bhat, G. S., and Coauthors, 2001: BOBMEX: The Bay of Bengal Monsoon Experiment. *Bull. Amer. Meteor. Soc.,* **82,** 2217–2243, doi:10.1175/1520-0477(2001)082<2217:BTBOBM>2.3.CO;2.

Bourlès, B., and Coauthors, 2008: The PIRATA program: History, accomplishments, and future directions. *Bull. Amer. Meteor. Soc.,* **89,** 1111–1125, doi:10.1175/2008BAMS2462.1.

Cai, S., X. Long, R. Wu, and S. Wang, 2008: Geographical and monthly variability of the first baroclinic Rossby radius of deformation in the South China Sea. *J. Mar. Syst.,* **74,** 711–720, doi:10.1016/j.jmarsys.2007.12.008.

Chan, J. C. L., 1995: Prediction of annual tropical cyclone activity over the western North Pacific and the South China Sea. *Int. J. Climatol.,* **15,** 1011–1019, doi:10.1002/joc.3370150907.

——, and M. Xu, 2009: Inter-annual and inter-decadal variations of landfalling tropical cyclones in East Asia. Part I: Time series analysis. *Int. J. Climatol.*, **29,** 1285–1293, doi:10.1002/joc.1782.

Chen, F., Y. Du, L. Yan, D. Wang, and P. Shi, 2010: Response of upper ocean currents to typhoons at two ADCP moorings west of the Luzon Strait. *Chin. J. Oceanol. Limnol.,* **28,** 1002–1011, doi:10.1007/s00343-010-0025-z.

Chen, G., Y. Hou, X. Chu, P. Qi, and P. Hu, 2009: The variability of eddy kinetic energy in the South China Sea deduced from satellite altimeter data. *Chin. J. Oceanol. Limnol.,* **27,** 943–954, doi:10.1007/s00343-009-9297-6.

——, ——, Q. Zhang, and X. Chu, 2010: The eddy pair off eastern Vietnam: Interannual variability and

impact on thermohaline structure. *Cont. Shelf Res.,* **30,** 715–723, doi:10.1016/j.csr.2009.11.013.

——, ——, and X. Chu, 2011: Mesoscale eddies in the South China Sea: Mean properties, spatio-temporal variability and impact on thermohaline structure. *J. Geophys. Res.,* **116,** C06018, doi:10.1029/2010JC006716.

——, J. Gan, Q. Xie, X. Chu, D. Wang, and Y. Hou, 2012: Eddy heat and salt transports in the South China Sea and their seasonal modulations. *J. Geophys. Res.,* **117,** C05021, doi:10.1029/2011JC007724.

Cheng, X., and Y. Qi, 2010: Variations of eddy kinetic energy in the South China Sea. *J. Oceanogr.,* **66,** 85–94, doi:10.1007/s10872-010-0007-y.

Chow, C. H., and Q. Liu, 2012: Eddy effects on sea surface temperature and sea surface wind in the continental slope region of the northern South China Sea. *Geophys. Res. Lett.,* **39,** L02601, doi:10.1029/2011GL050230.

Chu, P., and C. Fan, 2001: A low salinity cool-core cyclonic eddy detected northwest of Luzon during the South China Sea Monsoon Experiment (SCSMEX) in July 1998. *J. Oceanogr.,* **57,** 549–563, doi:10.1023/A:1021251519067.

Chu, X., H. Xue, Y. Qi, G. Chen, Q. Mao, D. Wang, and F. Chai, 2014: An exceptional anticyclonic eddy in the South China Sea in 2010. *J. Geophys. Res. Oceans,* **119,** 881–897, doi:10.1002/2013JC009314.

Curry, J. A., and Coauthors, 2004: SEAFLUX. *Bull. Amer. Meteor. Soc.,* **85,** 409–424, doi:10.1175/BAMS-85-3-409.

Dahlin, H., 1997: Towards a Baltic operational oceanographic system, "BOOS." *Operational Oceanography: The Challenge for European Co-operation,* J. H. Stel et al., Eds., Elsevier Oceanography Series, Vol. 62, Elsevier, 331–335.

Dale, W. L., 1956: Wind and drift currents in the South China Sea. *Malays. J. Trop. Geogr.,* **8,** 1–31.

Ding, Y., and Y. Liu, 2001: Onset and the evolution of the summer monsoon over the South China Sea during the SCSMEX field experiment in 1998. *J. Meteor. Soc. Japan,* **79,** 255–276, doi:10.2151/jmsj.79.255.

——, C. Li, and Y. Liu, 2004: Overview of the South China Sea Monsoon Experiment. *Adv. Atmos. Sci.,* **21,** 343–360, doi:10.1007/BF02915563.

Dippner, J., K. Nguyen, H. Hein, T. Ohde, and N. Loick, 2007: Monsoon-induced upwelling off the Vietnamese coast. *Ocean Dyn.,* **57,** 46–62, doi:10.1007/s10236-006-0091-0.

Du, Y., S.-P. Xie, G. Huang, and K. Hu, 2009: Role of air–sea interaction in the long persistence of El Niño–induced north Indian Ocean warming. *J. Climate,* **22,** 2023–2038, doi:10.1175/2008JCLI2590.1.

Duce, R. A., and P. S. Liss, 2002: The Surface Ocean—Lower Atmosphere Study (SOLAS). *Atmos. Environ.,* **36,** 5119–5120, doi:10.1016/S1352-2310(02)00327-8.

Edson, J., and Coauthors, 2007: The coupled boundary layers and air–sea transfer experiment in low winds. *Bull. Amer. Meteor. Soc.,* **88,** 341–356, doi:10.1175/BAMS-88-3-341.

Fairall, C. W., E. F. Bradley, D. P. Rogers, J. B. Edson, and G. S. Young, 1996: Bulk parameterization of air-sea fluxes for Tropical Ocean-Global Atmosphere Coupled-Ocean Atmosphere Response Experiment. *J. Geophys. Res.,* **101,** 3747–3764, doi:10.1029/95JC03205.

Fang, W., G. Fang, P. Shi, Q. Huang, and Q. Xie, 2002: Seasonal structures of upper layer circulation in the southern South China Sea from in situ observations. *J. Geophys. Res.,* **107,** 3202, doi:10.1029/2002JC001343.

Fujita, T. T., 1981: Tornadoes and downbursts in the context of generalized planetary scales. *J. Atmos. Sci.,* **38,** 1511–1534.

Fujita, M., K. Yoneyama, S. Mori, T. Nasuno, and M. Satoh, 2011: Diurnal convection peaks over the eastern Indian Ocean off Sumatra during different MJO phases. *J. Meteor. Soc. Japan,* **89A,** 317–330, doi:10.2151/jmsj.2011-A22.

Gan, J., and T. Qu, 2008: Coastal jet separation and associated flow variability in the southwest South China Sea. *Deep-Sea Res. I,* **55,** 1–19, doi:10.1016/j.dsr.2007.09.008.

——, H. Li, E. Curchitser, and D. Haidvogel, 2006: Modeling South China Sea circulation: Response to seasonal forcing regimes. *J. Geophys. Res.,* **111,** C06034, doi:10.1029/2005JC003298.

——, A. Cheung, X. Guo, and L. Li, 2009: Intensified upwelling over a widened shelf in the northeastern South China Sea. *J. Geophys. Res.,* **114,** C09019, doi:10.1029/2007JC004660.

Guan, B., 1985: Some features of the temporal and spatial distributions of the "counter-wind" current in northern South China Sea in winter (in Chinese). *Oceanol. Limnol. Sin.,* **16,** 429–438.

——, and S. Chen, 1964: *Ocean Current System in East China Sea and South China Sea* (in Chinese). National Marine Survey Rep., 88 pp.

Guan, L., and H. Kawamura, 2004: Merging satellite infrared and microwave SST-methodology and evaluation of the new SST. *J. Oceanogr.,* **60,** 905–912, doi:10.1007/s10872-005-5782-5.

He, Z., D. Wang, and J. Hu, 2002: Features of eddy kinetic energy and variations of upper circulation in the South China Sea. *Acta Oceanol. Sin.,* **21** (2), 305–314.

——, Y. Zhang, and D. Wang, 2013: Spring mesoscale high in the western South China Sea. *Acta Oceanol. Sin.,* **32,** 1–5, doi:10.1007/s13131-013-0318-0.

Ho, C.-R., Q. Zheng, Y. S. Soong, N. Kuo, and J. Hu, 2000: Seasonal variability of sea surface height in the South China Sea observed with TOPEX/Poseidon altimeter data. *J. Geophys. Res.,* **105,** 13 981–13 990, doi:10.1029/2000JC900001.

Hu, J., H. Kawamura, H. Hong, and Y. Qi, 2000: A review on the currents in the South China Sea: Seasonal circulation, South China Sea warm current and Kuroshio intrusion. *J. Oceanogr.,* **56,** 607–624, doi:10.1023/A:1011117531252.

Huang, J., and P.-W. Chan, 2011: Progress of marine meteorological observation experiment at Maoming of South China. *J. Trop. Meteor.,* **17,** 418–429, doi:10.3969/j.issn.1006-8775.2011.04.012.

Huo, D., S. Li, and C. Xu, 2012: Service system of the South China Sea science data products based on VisualDB (in Chinese with English abstract). *J. Trop. Oceanogr.,* **31** (2), 118–122.

Jing, Z., Y. Qi, Z. Hua, and H. Zhang, 2009: Numerical study on the summer upwelling system in the northern continental shelf of the South China Sea. *Cont. Shelf Res.,* **29,** 467–478, doi:10.1016/j.csr.2008.11.008.

Klein, S. A., B. J. Soden, and N-C. Lau, 1999: Remote Sea Surface Temperature Variations during ENSO: Evidence for a Tropical Atmospheric Bridge. *J. Climate,* **12,** 917–932.

Koblinsky, C. J., J. J. Simpson, and T. D. Dickey, 1984: An offshore eddy in the California current system part II: Surface manifestation. *Prog. Oceanogr.,* **13,** 51–69, doi:10.1016/0079-6611(84)90005-3.

Kuo, N., Q. Zheng, and C. R. Ho, 2000: Satellite observation of upwelling along the western coast of the South China Sea. *Remote Sens. Environ.,* **74,** 463–470, doi:10.1016/S0034-4257(00)00138-3.

Kuroda, Y., and Y. Amitani, 2000: TRITON: New ocean and atmospheric observing buoy network for monitoring ENSO. *Umi no Kenkyu,* **10,** 157–172.

Lau, K. M., and Coauthors, 2000: A report of the field operations and early results of the South China Sea Monsoon Experiments (SCSMEX). *Bull. Amer. Meteor. Soc.,* **81,** 1261–1270, doi:10.1175/1520-0477(2000)081<1261:AROTFO>2.3.CO;2.

Lestari, R. K., M. Watanabe, and M. Kimoto, 2011: Role of air-sea coupling in the interannual variability of the South China Sea summer monsoon. *J. Meteor. Soc. Japan,* **89A,** 283–290, doi:10.2151/jmsj.2011-A18.

Li, C., Y. Zhang, and D. Wang, 2006: Impact of cold surges on sea surface temperature in the South China Sea in autumn of 2004 (in Chinese with English abstract). *J. Trop. Oceanogr.,* **25** (2), 6–11.

Li, J., D. Wang, J. Chen, and L. Yang, 2012: Comparison of remote sensing data with in-situ wind observation during the development of the South China Sea monsoon (in Chinese). *J. Oceanol. Limnol.,* **30,** 933–943, doi:10.1007/s00343-012-1285-6.

Li, Y., S. Peng, J. Wang, and J. Yan, 2014: Impacts of nonbreaking wave-stirring-induced mixing on the upper ocean thermal structure and typhoon intensity in the South China Sea. *J. Geophys. Res. Oceans,* **119,** 5052–5070, doi:10.1002/2014JC009956.

Liao, G., Y. Yuan, and X. Xu, 2007: Diagnostic calculation of the circulation in the South China Sea during summer 1998. *J. Oceanogr.,* **63,** 161–178, doi:10.1007/s10872-007-0019-4.

——, ——, and ——, 2008: Three dimensional diagnostic study of the circulation in the South China Sea during winter 1998. *J. Oceanogr.,* **64,** 803–814, doi:10.1007/s10872-008-0067-4.

Lin, P., W. Fang, Y. Chen, and X. Tang, 2007: Temporal and spatial variation characteristics on eddies in the South China Sea I. Statistical analyses (in Chinese with English abstract). *Acta Oceanol. Sin.,* **29** (3), 14–22.

Liu, C., D. Wang, J. Chen, Y. Du, and Q. Xie, 2012: Freshening of the intermediate water of the South China Sea between the 1960s and the 1980s. *Chin. J. Oceanol. Limnol.,* **30,** 1010–1015, doi:10.1007/s00343-012-1280-y.

Liu, Q., R. Huang, D. Wang, Q. Xie, and Q. Huang, 2006: Interplay between the Indonesian Throughflow and the South China Sea Throughflow. *Chin. Sci. Bull.,* **51,** 50–58, doi:10.1007/s11434-006-9050-x.

Liu, W. T., 1986: Statistical relation between monthly mean precipitable water and surface-level humidity over global oceans. *Mon. Wea. Rev.,* **114,** 1591–1601, doi:10.1175/1520-0493(1986)114<1591:SRBMMP>2.0.CO;2.

Liu, X., J. Wang, X. Cheng, and Y. Du, 2012: Abnormal upwelling and chlorophyll-*a* concentration off South Vietnam in summer 2007. *J. Geophys. Res.,* **117,** C07021, doi:10.1029/2012JC008052.

Liu, Y., and Y. Ding, 2003: Simulation of activity of the Asian summer monsoon and heavy rainfalls in China in 1998 with regional climate model. *Acta Meteor. Sin.,* **17** (Suppl.), 273–288.

——, ——, and Y. Song, 2011: Relationship between the Meiyu over the Yangtze-Huaihe River basins and the frequencies of tropical cyclone genesis in the western North Pacific. *J. Meteor. Soc. Japan,* **89A,** 141–152, doi:10.2151/jmsj.2011-A09.

Long, X., S. Wang, X. Shang, R. Chen, and D. Wang, 2010: Monitoring disastrous hydro-meteorological environment related to typhoon around the Xisha Islands (in Chinese). *J. Trop. Oceanogr.,* **29** (6), 29–33.

Ma, Y., Y. Wang, L. Zhang, R. Wu, S. Wang, and M. Li, 2011: The characteristics of atmospheric turbulence

and radiation energy transfer and the structure of atmospheric boundary layer over the northern slope area of Himalaya. *J. Meteor. Soc. Japan,* **89A,** 345–353, doi:10.2151/jmsj.2011-A24.

McPhaden, M. J., and Coauthors, 1998: The Tropical Ocean-Global Atmosphere (TOGA) observing system: A decade of progress. *J. Geophys. Res.,* **103,** 14 169–14 240, doi:10.1029/97JC02906.

McPhaden, M. J., and Coauthors, 2009: RAMA: The Research Moored Array for African–Asian–Australian monsoon analysis and prediction. *Bull. Amer. Meteor. Soc.,* **90,** 459–480, doi:10.1175/2008BAMS2608.1.

Mentes, S. S., and Z. Kaymaz, 2007: Investigation of surface duct conditions over Istanbul, Turkey. *J. Appl. Meteor. Climatol.,* **46,** 318–337, doi:10.1175/JAM2452.1.

Nan, F., Z. He, H. Zhou, and D. Wang, 2011: Three long-lived anticyclonic eddies in the northern South China Sea. *J. Geophys. Res.,* **116,** C05002, doi:10.1029/2010JC006790.

——, H. Xue, F. Chai, D. Wang, F. Yu, M. Shi, P. Guo, and P. Xiu, 2013: Weakening of the Kuroshio intrusion into the South China Sea over the past two decades. *J. Climate,* **26,** 8097–8110, doi:10.1175/JCLI-D-12-00315.1.

Nash, J., T. Oakley, H. Vömel, and W. Li, 2011: WMO intercomparison of high quality radiosonde observing systems: Yangjiang, China, 12 July–3 August 2010. World Meteorological Organization Instruments and Observing Methods Rep. 107, 238 pp.

Ou, S., H. Zhang, and D. Wang, 2009: Dynamics of the buoyant plume off the Pearl River estuary in summer. *Environ. Fluid Mech.,* **9,** 471–492, doi:10.1007/s10652-009-9146-3.

Peng, S., D. Liu, Z. Sun, and Y. Li, 2012: Recent advances in regional air-sea coupled models. *China Earth Sci.,* **55,** 1391–1405, doi:10.1007/s11430-012-4386-3.

Qin, H., G. Chen, W. Wang, D. Wang, and L. Zeng, 2014: Validation and application of MODIS-derived SST in the South China Sea. *Int. J. Remote Sens.,* **35,** 4315–4328, doi:10.1080/01431161.2014.916439.

Qiu, C., D. Wang, H. Kawamura, L. Guan, and H. Qin, 2009: Validation of AVHRR and TMI-derived sea surface temperature in the northern South China Sea. *Cont. Shelf Res.,* **29,** 2358–2366, doi:10.1016/j.csr.2009.10.009.

Qu, T., 2000: Upper-layer circulation in the South China Sea. *J. Phys. Oceanogr.,* **30,** 1450–1460, doi:10.1175/1520-0485(2000)030<1450:ULCITS>2.0.CO;2.

——, Y. Du, G. Meyers, A. Ishida, and D. Wang, 2005: Connecting the tropical Pacific with Indian Ocean through South China Sea. *Geophys. Res. Lett.,* **32,** L24609, doi:10.1029/2005GL024698.

——, ——, and H. Sasaki, 2006: South China Sea Throughflow: A heat and freshwater conveyor. *Geophys. Res. Lett.,* **33,** L23617, doi:10.1029/2006GL028350.

Ren, X., and Y. Qian, 2001: Development of a coupled regional air-sea model and its numerical simulation for summer monsoon in 1998. *Acta Meteor. Sin.,* **15,** 385–396.

Rudnick, D. L., R. E. Davis, C. C. Eriksen, D. M. Fratantoni, and M. J. Perry, 2004: Underwater gliders for ocean research. *Mar. Technol. Soc. J.,* **38,** 73–84, doi:10.4031/002533204787522703.

Sanjeeva Rao, P., and D. R. Sikka, 2005: Intraseasonal variability of the summer monsoon over the north Indian Ocean as revealed by the BOBMEX and ARMEX field programs. *Pure Appl. Geophys.,* **162,** 1481–1510, doi:10.1007/s00024-005-2680-0.

Shi, R., X. Guo, D. Wang, L. Zeng, and J. Chen, 2014: Seasonal variability in coastal fronts and its influence on sea surface wind in the northern South China Sea. *Deep-Sea Res. I,* doi:10.1016/j.dsr2.2013.12.018, in press.

——, L. Zeng, D. Wang, J. Chen, L. Yang, Y. He, D. Liu, and J. Yao, 2015: Observation and numerical simulation of the marine meteorology elements and air-sea fluxes at Yongxing Island in September 2013. *Aquat. Ecosyst. Health Manage.,* in press.

Shu, Y., D. Wang, J. Zhu, and S. Peng, 2011a: The 4-D structure of upwelling and Pearl River plume in the northern South China Sea during summer 2008 revealed by a data assimilation model. *Ocean Modell.,* **36,** 228–241, doi:10.1016/j.ocemod.2011.01.002.

——, J. Zhu, D. Wang, and X. Xiao, 2011b: Assimilating remote sensing and in situ observations into a coastal model of northern South China Sea using ensemble Kalman filter. *Cont. Shelf Res.,* **31,** S24–S36, doi:10.1016/j.csr.2011.01.017.

Siedler, G., J. Church, and J. Gould, 2001: *Ocean Circulation and Climate: Observing and Modelling the Global Ocean.* International Geophysics Series, Vol. 77, Academic Press, 715 pp.

Small, R. J., and Coauthors, 2008: Air–sea interaction over ocean fronts and eddies. *Dyn. Atmos. Oceans,* **45,** 274–319, doi:10.1016/j.dynatmoce.2008.01.001.

Su, J., 2004: Overview of the South China Sea circulation and its influence on the coastal physical oceanography near the Pearl River estuary. *Cont. Shelf Res.,* **24,** 1745–1760, doi:10.1016/j.csr.2004.06.005.

——, and T. Pohlmann, 2009: Wind and topography influence on an upwelling system at the eastern Hainan coast. *J. Geophys. Res.,* **114,** C06017, doi:10.1029/2008JC005018.

Tippett, M. K., A. G. Barnston, D. G. DeWitt, and R.-H. Zhang, 2005: Statistical correction of tropical Pacific

sea surface temperature forecasts. *J. Climate,* **18,** 5141–5162, doi:10.1175/JCLI3581.1.

Todd, R. E., D. L. Rudnick, R. E. Davis, and M. D. Ohman, 2011: Underwater gliders reveal rapid arrival of El Niño effects off California's coast. *Geophys. Res. Lett.,* **38,** L03609, doi:10.1029/2010GL046376.

Tozuka, T., T. D. Qu, and T. Yamagata, 2007: Dramatic impact of the South China Sea on the Indonesian Throughflow. *Geophys. Res. Lett.,* **34,** L12612, doi:10.1029/2007GL030420.

Wang, C., W. Wang, D. Wang, and Q. Wang, 2006: Interannual variability of the South China Sea associated with El Niño. *J. Geophys. Res.,* **111,** C03023, doi:10.1029/2005JC003333.

Wang, D., Q. Xie, Y. Du, W. Wang, and J. Chen, 2002: The 1997–1998 warm event in the South China Sea. *Chin. Sci. Bull.,* **47,** 1221–1227, doi:10.1007/BF02907614.

——, B. Hong, J. Gan, and H. Xu, 2010a: Numerical investigation on propulsion of the counter-wind current in the northern South China Sea in winter. *Deep-Sea Res. I,* **57,** 1206–1221, doi:10.1016/j.dsr.2010.06.007.

——, W. Zhou, X. Yu, Q. Xie, and X. Wang, 2010b: Marine atmospheric boundary layers associated with summer monsoon onset over the South China Sea in 1998. *Atmos. Oceanic Sci. Lett.,* **3,** 263–270.

——, J. Li, L. Yang, and Y. He, 2012: The variations of atmospheric variables recorded at Xisha station in the South China Sea during tropical cyclone passages. *Advances in Hurricane Research—Modelling, Meteorology, Preparedness and Impacts,* K. Hickey, Ed., INTECH, doi:10.5772/50897.

——, Q. Wang, W. Zhou, S. Cai, L. Li, and B. Hong, 2013a: An analysis of the current deflection around Dongsha Islands in the northern South China Sea. *J. Geophys. Res. Oceans,* **118,** 490–501, doi:10.1029/2012JC008429.

——, L. Zeng, X. Li, and P. Shi, 2013b: Validation of satellite-derived daily latent heat flux over the South China Sea, compared with observations and five products. *J. Atmos. Oceanic Technol.,* **30,** 1820–1832, doi:10.1175/JTECH-D-12-00153.1.

——, Y. Shu, H. Xue, J. Hu, J. Chen, W. Zhuang, T. Zu, and J. Xu, 2014: Relative contributions of local wind and topography to the coastal upwelling intensity in the northern South China Sea. *J. Geophys. Res. Oceans,* **119,** 2550–2567, doi:10.1002/2013JC009172.

Wang, G., D. Chen, and J. L. Su, 2006: Generation and life cycle of the dipole in the South China Sea summer circulation. *J. Geophys. Res.,* **111,** C06002, doi:10.1029/2005JC003314.

Wang, H., Y. Yuan, W. Guan, R. Lou, and K. Wang, 2004: Circulation in the South China Sea during summer 2000 as obtained from observations and a generalized topography-following ocean model. *J. Geophys. Res.,* **109,** C07007, doi:10.1029/2003JD004119.

Wang, W., and C. Wang, 2006: Formation and decay of the spring warm pool in the South China Sea. *Geophys. Res. Lett.,* **33,** L02615, doi:10.1029/2005GL025097.

Wang, X., W. Li, Y. Qi, and G. Han, 2012: Heat, salt and volume transports by eddies in the vicinity. *Deep-Sea Res. I,* **61,** 21–33, doi:10.1016/j.dsr.2011.11.006.

Wang, Z., and L. Fei, 1987: *Manual for Typhoon Prediction* (in Chinese). China Meteorology Press, 360 pp.

Webster, P. J., and Coauthors, 2002: The JASMINE pilot study. *Bull. Amer. Meteor. Soc.,* **83,** 1603–1630, doi:10.1175/BAMS-83-11-1603.

Wentz, F. J., C. L. Gentemann, and D. Smith, 2000: Satellite measurements of sea surface temperature through clouds. Science, **288,** 847–850.

Wu, R., Z. When, S. Yang, and Y. Li, 2010: An interdecadal change in southern China summer rainfall around 1992/93. *J. Climate,* **23,** 2389–2403, doi:10.1175/2009JCLI3336.1.

Wu, P., Y. Fukutomi, and J. Matsumoto, 2011: An observational study of the extremely heavy rain event in northern Vietnam during 30 October-1 November 2008. *J. Meteor. Soc. Japan,* **89A,** 331–344, doi:10.215/jmsj.2011-A23.

Wyrtki, K., 1961: Physical oceanography of Southeast Asia waters. Scripps Institute of Oceanography NAGA Rep. 2, 195 pp.

Xie, Q., K. Huang, D. Wang, L. Yang, J. Chen, Z. Wu, D. Li, and Z. Liang, 2014: An intercomparison of GPS radiosonde soundings during the eastern tropical Indian Ocean experiment. *Acta Oceanol. Sin.,* **33,** 127–134, doi:10.1007/s13131-014-0422-9.

Xie, S.-P., Q. Xie, D. Wang, and W. T. Liu, 2003: Summer upwelling in the South China Sea and its role in regional climate variations. *J. Geophys. Res.,* **108,** 3261, doi:10.1029/2003JC001867.

——, C.-H. Chang, Q. Xie, and D. Wang, 2007: Intraseasonal variability in the summer South China Sea: Wind jet, cold filament, and recirculations. *J. Geophys. Res.,* **112,** C10008, doi:10.1029/2007JC004238.

——, K. M. Hu, J. Hafner, H. Tokinaga, Y. Du, G. Huang, and T. Sampe, 2009: Indian Ocean capacitor effect on Indo–western Pacific climate during the summer following El Niño. *J. Climate,* **22,** 730–747, doi:10.1175/2008JCLI2544.1.

Xu, C., S. Li, and P. Mi, 2010: OPeNDAP service based implementation of physical oceanographic data of the South China Sea (in Chinese with English abstract). *J. Trop. Oceanogr.,* **29** (4), 174–180.

Xu, G., and Q. Zhu, 2002: Feature analysis of summer monsoon LFO over SCS in 1998. *J. Trop. Meteor.,* **18,** 309–316.

Xue, H., F. Chai, D. Xu, and M. Shi, 2001: Characteristics and seasonal variation of the coastal current in the South China Sea (in Chinese). *Oceanogr. China,* **13,** 64–75.

——, ——, N. Pettigrew, D. Xu, M. Shi, and J. Xu, 2004: Kuroshio intrusion and the circulation in the South China Sea. *J. Geophys. Res.,* **109,** C02017, doi:10.1029/2002JC001724.

Yang, J., Q. Liu, S.-P. Xie, Z. Liu, and L. Wu, 2007: Impact of the Indian Ocean SST basin mode on the Asian summer monsoon. *Geophys. Res. Lett.,* **34,** L02708, doi:10.1029/2006GL028571.

Yang, L., Y. Du, S.-P. Xie, and D. Wang, 2012: An interdecadal change of tropical cyclone activity in the South China Sea in the early 1990s. *Chin. J. Oceanol. Limnol.,* **30,** 138–144, doi:10.1007/s00343-012-1258-9.

——, ——, D. Wang, C. Wang, and X. Wang, 2015: Impact of intraseasonal oscillation on the tropical cyclone track in the South China Sea. *Climate Dyn.,* **44,** 1505–1519, doi:10.1007/s00382-014-2180-y.

Yuan, D. L., W. Q. Han, and D. X. Hu, 2007: Anticyclonic eddies northwest of Luzon in summer–fall observed by satellite altimeters. *Geophys. Res. Lett.,* **34,** L13610, doi:10.1029/2007GL029401.

Yuan, Y. C., G. H. Liao, and C. G. Yang, 2008: The Kuroshio near the Luzon Strait and circulation in the northern South China Sea during August and September 1994. *J. Oceanogr.,* **64,** 777–788, doi:10.1007/s10872-008-0065-6.

Zeng, L., P. Shi, W. T. Liu, and D. Wang, 2009: Evaluation of a satellite-derived latent heat flux product in the South China Sea: A comparison with moored buoy data and various products. *Atmos. Res.,* **94,** 91–105, doi:10.1016/j.atmosres.2008.12.007.

——, X. Li, Y. Du, R. Shi, J. Yao, D. Wang, and D. Sui, 2012: Synoptic-scale disturbances over the northern South China Sea and their responses to El Niño. *Acta Oceanol. Sin.,* **31,** 69–78, doi:10.1007/s13131-012-0237-5.

——, W. T. Liu, H. Xue, P. Xiu and D. Wang, 2014: Freshening in the South China Sea during 2012 revealed by Aquarius and in situ data. *J. Geophys. Res. Oceans,* **119,** 8296–8314, doi:10.1002/2014JC010108.

Zeng, X., I. M. Belkin, S. Peng, and Y. Li, 2014: East Hainan upwelling fronts detected by remote sensing and modelled in summer. *Int. J. Remote Sens.,* **35,** 4441–4451, doi:10.1080/01431161.2014.916443.

Zhao, H., D. Tang, and D. Wang, 2009: Phytoplankton blooms near the Pearl River estuary induced by Typhoon Nuri. *J. Geophys. Res.,* **114,** C12027, doi:10.1029/2009JC005384.

Zhao, X., D. Wang, S. Huang, K. Huang, and J. Chen, 2013: Statistical estimations of atmospheric duct over the South China Sea and the tropical eastern Indian Ocean. *Chin. Sci. Bull.,* **58,** 2794–2797, doi:10.1007/s11434-013-5942-8.

Zhou, W., W. Chen, and D. Wang, 2012: The implications of ENSO signal for south China monsoon climate. *Aquat. Ecosyst. Health Manage.,* **15,** 14–19, doi:10.1080/14634988.2012.652050.

Zhuang, W., Y. Du, D. Wang, Q. Xie, and S.-P. Xie, 2010: Pathways of mesoscale variability in the South China Sea. *Chin. J. Oceanol. Limnol.,* **28,** 1055–1067, doi:10.1007/s00343-010-0035-x.

Zu, T., and J. Gan, 2015: A numerical study of coupled estuary–shelf circulation around the Pearl River estuary during summer: Responses to variable winds, tides and river discharge. *Deep-Sea Res. II,* **117,** 53–64, doi:10.1016/j.dsr2.2013.12.010.

SHOP

the new AMS online bookstore

Use this **easy-to-navigate** site to review and purchase new and classic titles in the collection of AMS Books—including general interest weather books, histories, biographies, and monographs—plus much more.

View tables of contents, information about the authors, and independent reviews.

As always, **AMS members receive deep discounts** on all AMS Books.

www.ametsoc.org/amsbookstore

The new AMS online bookstore is now open.

Booksellers and wholesale distributors may set up accounts with our distributor, The University of Chicago Press, by contacting Karen Hyzy at khyzy@press.uchicago.edu, 773-702-7000, or toll-free at 800-621-2736.

AMS BOOKS

RESEARCH | APPLICATIONS | HISTORY